

See discussions, stats, and author profiles for this publication at: <https://www.researchgate.net/publication/332648056>

Usability and challenges of offshore wind energy in Vietnam revealed by the regional climate model simulation

Article in *Scientific online letters on the atmosphere: SOLA* · April 2019

DOI: 10.2151/sola.2019-021

CITATIONS

0

READS

71

7 authors, including:



Van Q. Doan

Centre for Climate Research Singapore

18 PUBLICATIONS 36 CITATIONS

[SEE PROFILE](#)



Van-Nguyen Dinh

University College Cork

35 PUBLICATIONS 256 CITATIONS

[SEE PROFILE](#)



Hiroyuki Kusaka

University of Tsukuba

119 PUBLICATIONS 2,805 CITATIONS

[SEE PROFILE](#)



Cong Thanh

VNU University of Science

7 PUBLICATIONS 6 CITATIONS

[SEE PROFILE](#)

Some of the authors of this publication are also working on these related projects:



Vietnam marine economy [View project](#)



NC vật lý biển Đông-Physics of Vietnam Sea [View project](#)



The Meteorological
Society of
Japan

Scientific Online Letters on the Atmosphere (SOLA)

EARLY ONLINE RELEASE

This is a PDF of a manuscript that has been peer-reviewed and accepted for publication. As the article has not yet been formatted, copy edited or proofread, the final published version may be different from the early online release.

This pre-publication manuscript may be downloaded, distributed and used under the provisions of the Creative Commons Attribution 4.0 International (CC BY 4.0) license. It may be cited using the DOI below.

The DOI for this manuscript is

DOI: 10.2151/sola.2019-021.

J-STAGE Advance published date: Apr. 25, 2019

The final manuscript after publication will replace the preliminary version at the above DOI once it is available.

1 **Usability and challenges of offshore wind energy in Vietnam**
2 **revealed by the regional climate model simulation**

3 Van Q. Doan¹, Van Nguyen Dinh², Hiroyuki Kusaka³, Thanh Cong⁴, Ansar Khan⁵,

4 Toan Van Du⁶, Nguyen Dinh Duc⁷

5 ¹ *Center for Computational Sciences, University of Tsukuba, Tsukuba, Japan*

6 *(Current affiliation: Centre for Climate Research Singapore, Singapore)*

7 ² *MaREI Centre for Marine and Renewable Energy, University College Cork, Cork,*

8 *Ireland*

9 ³ *Center for Computational Sciences, University of Tsukuba, Tsukuba, Japan*

10 ⁴ *VNU Hanoi, University of Sciences, Hanoi, Vietnam*

11 ⁵ *Department of Geography, Lalbaba College, University of Calcutta, Kolkata, India*

12 ⁶ *Vietnam Institute of Seas and Islands, MONRE, Hanoi, Vietnam*

13 ⁷ *VNU Hanoi, University of Engineering and Technology, Hanoi, Vietnam*

14 Corresponding author: Van Q. Doan, Centre for Climate Research Singapore, 36 Kim

15 Chuan Rd, Singapore 537054. E-mail: doan_quang_van@nea.gov.sg

16

17 **Abstract**

18 This study revealed great potential and shortcoming of offshore wind energy in Vietnam
19 by numerical simulations with Weather Research and Forecasting (WRF) model at 10-
20 km resolution for 10 years (2006 – 2015). The greatest energy potential was found in the
21 offshore area of Phu Quy island (Binh Thuan province). The area, alone, can provide the
22 38.2 GW power generation capacity corresponding to the increasing renewable-energy
23 demand by 2030 planned by the country. There is also a drawback of the wind resource,
24 which is associated with strong multiple-scale temporal variabilities. The seasonal
25 variability associated with monsoon onsets and daily variability associated with the wind
26 diurnal cycles were found ranging 30 – 50 %. Meanwhile, the inter-annual variability
27 could reach up to 10 %. These variabilities must be considered when designing wind
28 farms and grids over the region. Additionally, due to the fact that the WRF model
29 performed climatological features of the winds well against the observations, this results
30 indicate that it can be useful tools for wind-power assessment as compared to other
31 reanalysis or QuikSCAT data with courser spatio-temporal resolutions.

32 **Keywords:** Offshore wind power, Vietnam sea, Weather Research and Forecast model.

33

34 **1. Introduction**

35 Vietnam has been experienced fast economic development during the last several decades
36 with the energy consumption increasing constantly year by year. Most of energy

37 consumptions now are provided by hydro- and fossil-fuel powers (GIZ 2016). However,
38 due to their negative impacts on environment and ecology, renewable energy resources,
39 in particular wind energy, are becoming important to maintain a sustainable development
40 of the country (Dinh and McKeogh 2018, Dinh and Nguyen 2018).

41 A drawback of wind energy is its high dependence on wind that fluctuates greatly at all
42 time scales: seconds, minutes, hours, days, months, seasons and years (Ohba et al. 2016,
43 Doan et al. 2019). Understanding wind temporal variations is of key importance for the
44 integration and optimal utilization of wind in the power system (Foley et al. 2012).
45 Recently, offshore wind has gained increasing attention because of its relatively higher
46 stability compared to onshore wind (Dvorak et al. 2010, Jacobson and Delucchi 2011),
47 and the technological improvement enables cutting the building cost of an offshore wind
48 farm.

49 The biggest issue of offshore wind resource assessment is a lack of observational wind
50 data, especially those at turbine heights (Mattar and Borvaran 2016). The observed wind
51 data, in most cases, are very limited in terms of time and space and they are difficult to
52 be used for assessing the wind potential for a broad region. Moreover, a precise
53 assessment requires wind data enabling to encompass a long enough time period with
54 high enough temporal frequency in order to capture the multiple-scale temporal
55 variabilities (Argüeso et al. 2018).

56 Assessment of offshore wind power in Vietnam may be difficult because, firstly, the
57 country has more than 3000 km of coastline, following the Truong Son mountain range
58 stretching from north to south. In many places, the complex coast's terrain can affect the
59 distribution of offshore winds. Secondly, the country is located in the tropical monsoon
60 region with two distinct wind directions, southwest in the summer months and northeast
61 in the winter months. The annual cycle of seasons implies a strong variability in winds
62 putting a challenge on the stable and efficient operation of wind power plants.

63 Recently, numerical modelling approach with regional climate models (RCMs) has been
64 adopted to assess the offshore wind recourses. RCMs are powerful to generate complete
65 and physically consistent wind data. RCMs allow to estimate winds at given turbine-hub
66 heights, they can also reproduce long-term time series of high frequency outputs, both in
67 time and space. Some successful examples of the modeling approach for assessing wind
68 power potential are Carvalho et al. (2014) for Portugal, Nawri et al. (2014) for Ireland,
69 Yamaguchi et al. (2014) for Japan, Mattar et al. (2016) for Chile, Fant et al. (2016) for
70 South Africa, Giannaros et al. (2017) for Greece, and Argüeso et al. (2018) for Hawaii,
71 USA.

72 However, none of such above studies having focused on the offshore wind energy in the
73 Southeast Asia. One exception is the recent study of Doan et al. (2018) that has attempted
74 to simulate the offshore wind over the area limited to the Southern Vietnam using a RCM.
75 However, in their study, the simulated wind data have not been validated against
76 observations. It is still unknown how the numerical modelling approach can perform the

77 wind climate in this region. Besides, even though the numerical simulations in the
78 previous studies are valuable assessing the offshore wind potential, none other than that
79 of Argueso et al. (2018) was run over periods that exceeded a year, thus, they do not
80 provide data on the long-term variability and may lack statistical robustness for wind
81 energy analysis. These study gaps need to be filled. On the other hand, from a practical
82 point of view, the assessment of offshore wind resources in Vietnam is also an urgent
83 issue to cope with the rapidly increasing renewable-energy demand associated with
84 economic development.

85 This study assesses the offshore-wind-power potential over the sea of Vietnam using a
86 state-of-art regional climate model, the Weather Research and Forecasting (WRF) model.
87 The numerical simulation is run for 10-year period (2006 – 2015) with the finest
88 resolution of 10 x 10 km that cover whole the Vietnam region to have robust wind data
89 for analyzing. The variabilities of wind power potential in space and time at multiple scale
90 from inter-annual to hourly are fully characterized. To the best of our knowledge, this is
91 the first study describing the offshore wind power generation capacity in the Vietnam
92 region from the climatological view using a numerical method. The results obtained will
93 be useful for the policy makers as well as developers seeking optimal placement of
94 offshore wind farms.

95 **2. Methods**

96 **2.1 Atmospheric model and simulation design**

97 The Weather Research and Forecast (WRF) model version 3.5.1 was used to reproduce
98 the wind climate over the Vietnam region. Model configurations are shown in Table 1.

99 The model includes two nested grids with grid spacing of the inner most domain 10 x 10
100 km (Fig. 1). Slide runs (for each month) was conducted for ten years 2006 Jan – 2015

101 Dec with the initial and boundary conditions created from the Final (FNL) Operational
102 Global Analysis data of the National Center for Environmental Prediction (NCEP) as the

103 initial and boundary conditions. The NCEP FNL data, which are provided every 6 hours,
104 have horizontal resolution of 1 x 1 degree (NCEP 2000). The 10-year simulation period

105 is expected to provide robust enough results to characterize the spatial and seasonal
106 variability of wind field over the region.

107 The physical schemes is chosen for popularity in wind simulation that was confirmed in
108 many previous studies (Argüeso et al. 2018). The Yonsei University (YSU) Planetary

109 Boundary Layer (PBL) scheme (Hong et al. 2006) was used to represent the turbulence
110 in the atmosphere boundary layer. The WRF Single-Moment 6-Class Microphysics

111 (WSM-6) scheme (Hong and Lim 2006) was chosen to solve cloud microphysics
112 processes. The Rapid Radiative Transfer Model (RRTM) for longwave radiation and the

113 Dudhia scheme for shortwave radiation were used for their efficiency and good
114 performance for wind simulations (Guo and Xiao 2014, Santos-Alamillos et al. 2013).

115 Convective processes were represented with the Kain-Fritsch cumulus scheme (Kain

116 2004) for two simulation domains. The Noah Land Surface Model (Chen and Dudhia
117 2001) was used to simulate the land-atmosphere interactions.

118 **2.2 Observation data**

119 The simulated wind speed was compared to the observational data to evaluate the
120 performance of the WRF model. Two observational data sources were used in this study.
121 The first is the wind data observed at six ground-based weather stations run by the
122 Vietnam Center of Hydro-Meteorological Data (VCHMD). Such stations are located in
123 islands off the coast of Vietnam (see Fig. 1b). The station data are measured four times
124 (00, 06, 12, 18 UTC) a day and available for 10 years 2006 – 2015.

125 Another source is the QuikSCAT (Quick Scatterometer) data. QuikSCAT is the NASA's
126 Earth observation satellite carrying the sea winds scatterometer (Draper et al. 2004, Said
127 et al. 2011). QuikSCAT provided the gridded wind speed with two components
128 referenced to 10 meters above the sea surface with global coverage at a spatial resolution
129 of 25 km. Only the data for five years 2006 – 2010 were used to compared to the simulated
130 data.

131 **2.3 Estimation of wind power potential**

132 Wind power density (WPD), a measure of energy flux through an area perpendicular to
133 the direction of motion, varies with the cube of wind speed and air density. WPD is the
134 defined as,

$$P_{den} = \frac{1}{2} \rho \frac{1}{N} \sum_{i=1}^N v_i^3, \quad (1)$$

135 where ρ is the air density assumed constant of $1.225 \text{ (kg/m}^3\text{)}$; v_i is instantaneous wind
136 speed; N is a total number of hours of the output wind speed data. Wind power density
137 depends on atmospheric variable and is therefore most appropriate for turbine-
138 independent evaluations of wind energy potential.

139 The turbine chosen for the hypothetical wind farm is Vestas V164-8.0. It has rated power
140 (P_r) of 8 MW with 80 m blade with swept area of $21,124 \text{ m}^2$. The approximate hub height
141 is 105 m. The turbine is used in use in several offshore wind farms such as Burbo Bank
142 Offshore, the United Kingdom and Norther N.V., Belgium (Aarhus, 2019). The turbine
143 starts generating power ($P_f(v)$) at the cut-in wind speed (v_{ci}), of 4 m/s and shuts off at
144 the cut-out wind speed (v_{co}) of 25 m/s. The rated wind speed (v_r) of the turbine is 13 m/s.
145 Using the hourly wind speed data and the power curve of the turbine (Fig. S1 in
146 Supplement), the hourly power production P_i from the turbine is calculated by using Eq.
147 (2).

$$P_i(v, t) = \begin{cases} 0, & v < v_{ci} \\ P_f(v), & v_{ci} \leq v < v_r \\ P_r, & v_r \leq v < v_{co} \\ 0, & v_{co} \leq v \end{cases} \quad (2)$$

148 The actual energy output (E) of the wind turbine for N hours can be calculated as

$$E = \sum_{i=1}^N P_i \quad (3)$$

149 where P_i is the hourly power production. N is number of hours.

150 **3. Results and discussions**

151 **3.1 Model validation**

152 Fig. 2 shows the probability distribution of the modeled and station observed wind speed.
153 The model, overall, appears to perform well the observed wind speed climate. Especially,
154 there is good matching in the shapes of probability distribution between the modelled and
155 the observed data, in particular, at Phu Quy, Truong Sa, Phu Quoc. However, it is likely
156 that there also exists positive biases (defined as the modelled result minus the observation)
157 over most stations, systematically. Biases range from 0.9 m/s at Phu Quoc to 3.5 m/s at
158 Phu Quy (Table 2). To explain these biases, it is worthwhile to remind that all 6 weather
159 stations are located in small islands of the Vietnam sea (Fig. 1b). However, having the
160 resolution of 10 x 10 km, the WRF model is unable to resolve these islands. The land use
161 categories of grid points, corresponding to the location of weather stations, were classified
162 as water surface rather than land (Table 2) in the model.

163 Additional sensitivity simulations with nesting to finer resolutions demonstrated that the
164 misrepresentation of island land use as water surface could induce underestimation of the
165 surface friction thus resulting in the overprediction of surface wind speed (Fig. S2 in

166 Supplements). This result is consistent with the finding by Santos-Alamillos (2015). On
167 the other hand, the wind speed at upper air levels has been predicted more consistently
168 by WRF at different resolutions (Fig. S2).

169 Fig. 3 shows the comparison between the modelled data and the QuikSCAT data. Much
170 better agreement between two wind speed datasets are seen, the biases are much smaller
171 than that when compared with station data. The mean bias of the WRF model versus the
172 QuikSCAT data was only 0.84 m/s (Fig. S3 in Supplements). The WRF model shows a
173 good performance in terms of either wind speed or direction. The seasonal variation,
174 which is due to the dominant northeastern monsoon during the winter months December
175 - January - February (DJF), and southwestern monsoon during summer months June -
176 July - August (JJA) was well predicted by the model. The lower wind speed in the inter-
177 monsoon months, March - April - May (MAM) and September – October – November
178 (SON) are seen in both the WRF and the QuikSCAT data. However, there is small
179 overestimation of wind speed during MAM.

180 The largest wind speed is seen in the offshore area of Phu Quy island (Binh Thuan
181 province in the south), followed by that of Bach Long Vi island (Quang Ninh province in
182 the north) (Fig. 4). The maximum surface wind speed at Phu Quy could reach 10 m/s in
183 DFJ; whereas, the maximum at Bach Long Vi was 9 m/s in SON.

184 **3.2 Wind power density**

185 The WPD calculated from the simulated wind speed at the hub height (105 m) is shown
186 in Fig. 4. Overall, the offshore wind power potential in Vietnam is characterized by the
187 strong heterogeneity both in space and time. The consistently high value is seen in the
188 area of the Phu Quy island where the WPD could reach above 2000 Wm^{-2} during DJF
189 (Fig. 4a) with the annual mean of 1200 Wm^{-2} (Fig. 5a). In the north, the higher value is
190 seen over the Bach Long Vi island, where it could reach above 1200 Wm^{-2} during SON
191 and the annual mean was greater than 1000 Wm^{-2} . The offshore areas of the northern and
192 central parts had the relatively lower WPD with the annual mean ranging 600 – 700 Wm^{-2}
193 (Fig. 5a). During inter-monsoon months, i.e., MAM and SON, the WPD was lower and
194 more spatially homogeneous (Fig. 4b, d).

195 Temporal variabilities of wind power generation is important in designing efficient wind
196 power plants. Here, the annual variability (Fig. 5b), i.e., the variation within the annual
197 cycle, of the WPD is defined as the normalized standard deviation of monthly means, the
198 daily variability (Fig. 5c) defined as the normalized standard deviation of hourly data
199 from the daily mean; the inter-annual variability (Fig. 5d) defined as the normalized
200 standard deviation of yearly means during 10-year period 2006 – 2015.

201 The variabilities at multiple temporal scales look more spatially identical. The annual
202 variability ranged 40 – 50 %, and the daily variability ranged 30 – 50 % (Fig. 5b, 5c). The
203 Southeast monsoon circulation, with dominant northeasterly wind during DJF and

204 southwesterly wind during JJA, is a reason for the annual variability of WPD over the
205 offshore area of Vietnam.

206 The comparison between the simulation versus the station observations and the
207 QuikSCAT data demonstrated the good performance on the annual and daily variabilities
208 (Fig. S4 and S5), though the model tended to overestimate the absolute WPD values. The
209 overestimation is seen in particular over Hon Ngu and Ly Son islands, which are located
210 relatively close to the land. Meanwhile, the model tended to underestimate WPD over
211 Truong Sa island which is located far away into the East Vietnam.

212 The inter-annual variability of WPD ranged 10 – 30 % lower than the annual and daily
213 variabilities. The inter-annual variability of WPD is strongly influenced by cross-
214 equatorial flow in the Indian ocean and negatively correlated with trade wind over the
215 western Pacific ocean during JJA. In contrast, it is highly affected by the Asia continent
216 high pressure during DJF (Fig. S6).

217 **3.3 Wind power generation**

218 Turbine Vestas V164-8.0, which has the hub height of 105 m and the rated power of 8
219 MW, was chosen for the hypothetical wind farm. The turbine is able to generate power at
220 the “effective” wind speed, i.e., between the cut-in 4 m/s and the cut-out 25 m/s.
221 Understanding the frequency, or fraction of “effective” wind speed to total time, is
222 important for efficient use of the wind turbine.

223 The simulated results show the strong variation of “effective” wind speed frequency over
224 space and time (Fig. S7). The highest frequency is seen over the offshore area of Binh
225 Thuan province, which could reach above 95 % in monsoon months, i.e., DFJ and JJA,
226 and being lower about 60 – 80 % in inter-monsoon months, i.e., MAM and SON.
227 Interestingly, the frequency was very high of 95 % over Phu Quoc island (southwestern
228 coast) in JJA. This was comparable with that over the offshore area of Binh Thuan
229 province, in spite of the lower the mean WPD observed here (Fig. 4c).

230 The wind power generation ability was analyzed. Assume the hypothetical turbines are
231 installed over the area of six islands (Fig. 6). The simulated result shows that the sea
232 areas of Bach Long Vi and Phu Quy islands can provide the power generation capacity
233 of 38.2 GW, which itself can contribute significantly to the national installed power
234 capacities of 60 GW in 2020 and 130 GW in 2030 as in the latest PDP in Vietnam (GIZ,
235 2016). Note that simulated wind power generation is likely higher than that calculated for
236 the QuikSCAT data (using power-law wind profile with an exponent of 0.11 for wind
237 over open water according to Hsu et al. 1993).

238 **4. Conclusions**

239 This study assessed the offshore-wind-power potential in the Vietnam sea by using the
240 numerical modelling approach with the WRF model. The findings revealed in this study
241 are described as following.

- 242 • Vietnam has high potential of offshore wind energy with the wind power density
243 greater than 400 W/m² in most offshore areas. However, the wind power potential
244 has strong spatial heterogeneity because of long and narrow geographical
245 characteristics of the country with more than 3000 km long south-north coastline.
246 The largest annual mean wind power density of above 1000 W/ m² was found near
247 to Phu Quy island (Binh Thuan province) and Bach Long Vi island (Quang Ninh
248 province). The area surrounding Phu Quy island, alone, can provide the power
249 generation capacity of 38.2 GW with the hypothetical wind turbine Vestas V164-
250 8.0.
- 251 • This study highlighted the drawback of offshore wind power associated with the
252 large temporal variabilities. The annual and daily variabilities are high about of
253 30 – 50 %. The inter-annual variability is about 10 – 30 %. These variabilities
254 should be carefully considered when designing wind farms and grids over the
255 region.
- 256 • The results obtained in this study can be a useful guideline for policy makers in
257 building the strategy of renewable energy infrastructure in Vietnam as well as for
258 developers who needs high-quality offshore wind power atlas to identify suitable
259 locations of wind farms. In addition, this highlighted the great potential using
260 numerical models for assessing the wind and wind power resources in Vietnam as
261 well as the other Southeast Asia countries in the tropical-monsoon climate zone
262 where lack of the offshore in-situ measurement network.

263 **Acknowledgement**

264 This work was supported by the “Interdisciplinary Computational Science Program” in
265 the Center for Computational Sciences, University of Tsukuba. The second author (V.N.
266 Dinh) has been funded by Science Foundation Ireland (SFI) Research Centre: MaREI -
267 Centre for Marine and Renewable Energy (12/RC/2302).

268 **Reference:**

269 Aarhus, 2019: World’s most powerful wind turbine selected for Belgium’s largest
270 offshore wind park (Available online at
271 <http://www.mhivestasoffshore.com/norther-foi/> accessed 12 April 2019)

272 Argüeso, D., and S. Businger, 2018: Wind power characteristics of Oahu, Hawaii.
273 *Renewable Energy*, **128**, 324-336.

274 Balog, I., P. M. Ruti, I. Tobin, V. Armenio, and R. Vautard, 2016: A numerical approach
275 for planning offshore wind farms from regional to local scales over the
276 Mediterranean. *Renewable Energy*, **85**, 395-405.

277 Carvalho, D., A. Rocha, M. Gómez-Gesteira, and C. S. Santos, 2014: WRF wind
278 simulation and wind energy production estimates forced by different reanalyses:
279 Comparison with observed data for Portugal. *Applied Energy*, **117**, 116-126.

- 280 Chen, F., and J. Dudhia, 2001: Coupling an advanced land surface-hydrology model with
281 the Penn State-NCAR MM5 modeling system. Part II : Preliminary model
282 validation. *Monthly Weather Review*, **129**(4), 587-604.
- 283 Dinh, V. N., and E. McKeogh, 2018: Offshore wind energy: technology opportunities and
284 challenges. *Lecture Notes in Civil Engineering, Proceedings of the Vietnam*
285 *Symposium on Advances in Offshore Engineering*, **18**, 3-22, doi: 10.1007/978-
286 981-13-2306-5_31.
- 287 Dinh, V. N., and H. X. Nguyen, 2018: Design of an offshore wind farm layout. *Lecture*
288 *Notes in Civil Engineering, Proceedings of the Vietnam Symposium on Advances*
289 *in Offshore Engineering*, **18**, 233-238, doi: 10.1007/978-981-13-2306-5_31.
- 290 Doan, V. Q., H. Kusaka, T. V. Du, D. D. Nguyen, and T. Cong, 2018: Numerical approach
291 for studying offshore wind power potential along the southern coast of Vietnam.
292 *Lecture Notes in Civil Engineering, Proceedings of the Vietnam Symposium on*
293 *Advances in Offshore Engineering*, **18**, 245-249.
- 294 Doan, V. Q., H. Kusaka, M. Matsueda, and R. Ikeda, 2019: Application of mesoscale
295 ensemble forecast method for prediction of wind speed ramps. *Wind Energy*, doi:
296 <https://doi.org/10.1002/we.2302>.

- 297 Draper, D. W., and D. G. Long, 2004: Evaluating the effect of rain on SeaWinds
298 scatterometer measurements. *Journal of Geophysical Research*, **109**, 1 – 12, doi:
299 10.1029/2002JC001741
- 300 Dvorak, M. J., C. L. Archer, and M. Z. Jacobson, 2010: California offshore wind energy
301 potential. *Renewable Energy*, **35(6)**, 1244-1254.
- 302 Fant, C., C. A. Schlosser, and K. Strzepek, 2016: The impact of climate change on wind
303 and solar resources in southern Africa. *Applied Energy*, **161**, 556-564.
- 304 Foley, A. M., P. G. Leahy, A. Marvuglia, and E. J. McKeogh, 2012: Current methods and
305 advances in forecasting of wind power generation. *Renewable Energy*, **37(1)**, 1-8.
- 306 Giannaros, T. M., D. Melas, and I. C. Ziomas, 2017: Performance evaluation of the
307 Weather Research and Forecasting (WRF) model for assessing wind resource in
308 Greece. *Renewable Energy*, **102**, 190-198.
- 309 Gesellschaft für Internationale Zusammenarbeit (GIZ), 2016: Vietnam Power
310 Development Plan for the Period 2011 - 2010: Highlights of the PDP 7 revised.
311 *GIZ Energy Support Programme in Viet Nam* (Available online at
312 <http://gizenergy.org.vn>)
- 313 Guo, Z., and X. Xiao, 2014: Wind power assessment based on a WRF wind simulation
314 with developed power curve modeling methods. *Abstract and Applied Analysis*,
315 **2014**, 1-15.

- 316 Hennessey, J., 1977: Some aspects of wind power statistics. *Journal of Applied*
317 *Meteorology*, **16(2)**, 119–128.
- 318 Hong, S., and J. Lim, 2006: The WRF single-moment 6-class microphysics scheme
319 (WSM6) . *Journal of the Korean Meteorological Society* , **42(2)**, 129-151.
- 320 Hong, S.-Y., Y. Noh, and J. Dudhia, 2006: A new vertical diffusion package with an
321 explicit treatment of entrainment processes. *Monthly Weather Review*, **134(9)**,
322 2318-2341.
- 323 Hsu, S. A., E. A. Meindl, and D. B. Gilhousen, 1994: Determining the power-law wind-
324 profile exponent under near-neutral stability conditions at sea . *Journal of Applied*
325 *Meteorology and Climatology*, **33**, 757-765.
- 326 Jacobson, M. Z., and M. A. Delucchi, 2011: Providing all global energy with wind, water,
327 and solar power, Part I: Technologies, energy resources, quantities and areas of
328 infrastructure, and materials. *Energy Policy*, **39(3)**, 1154-1169.
- 329 Kain, J. S., 2004: The Kain-Fritsch convective parameterization: an update. *Journal of*
330 *Applied Meteorology*, **43(1)**, 170-181.
- 331 Koplitz, S. N., D. J. Jacob, M. P. Sulprizio, L. Myllyvirta, and C. Reid, 2017: Burden of
332 disease from rising coal-fired power plant emissions in Southeast Asia.
333 *Environmental Science & Technology*, **51**, 1467 - 1476, doi:
334 10.1021/acs.est.6b03731.

- 335 Mattar, C., and D. Borvarán, D., 2016: Offshore wind power simulation by using WRF
336 in the central coast of Chile. *Renewable Energy*, **94**, 22-31.
- 337 National Centers for Environmental Prediction, 2000: *NCEP FNL Operational Model*
338 *Global Tropospheric Analyses, continuing from July 1999* (Available online at
339 <https://doi.org/10.5065/D6M043C6> accessed 12 April 2019)
- 340 Nawri, N., G. N. Petersen, H. Björnsson, A. N. Hahmann, K. Jónasson, C. B. Hasager,
341 and N. E. Clausen, 2014: The wind energy potential of Iceland. *Renewable Energy*,
342 **69**, 290-299.
- 343 Ohba, M., S. Kadokura, and D. Nohara, 2016: Impacts of synoptic circulation patterns on
344 wind power ramp events in East Japan. *Renewable Energy*, **96**, 591-602.
- 345 Said, F., and D. G. Long, 2011: Determining selected tropical cyclone characteristics
346 using QuikSCAT's ultra-high resolution images. *IEEE Journal of Selected Topics*
347 *in Applied Earth Observations and Remote Sensing*, **4(4)**, 857-869.
- 348 Santos-Alamillos, F. J., D. Pozo-Vázquez, J. A. Ruiz-Arias, V. Lara-Fanego, and J.
349 Tovar-Pescador, 2013: Analysis of WRF model wind estimate sensitivity to
350 physics parameterization choice and terrain representation in Andalusia (Southern
351 Spain). *Journal of Applied Meteorology and Climatology*, **52(7)**, 1592-1609.
- 352 Santos-Alamillos, F., D. Pozo-Vázquez, J. Ruiz-Arias, and J. Tovar-Pescador, 2015:
353 Influence of land-use misrepresentation on the accuracy of WRF wind estimates:

354 Evaluation of GLCC and CORINE land-use maps in southern Spain. *Atmospheric*
355 *Research*, **157**, 17 - 28.

356 Wind turbines database, 2019: Ventas V164-8.0 (Available online at [https://en.wind-](https://en.wind-turbine-models.com/turbines/318-vestas-v164-8.0)
357 [turbine-models.com/turbines/318-vestas-v164-8.0](https://en.wind-turbine-models.com/turbines/318-vestas-v164-8.0) accessed 12 April 2019).

358 Yamaguchi, A., and T. Ishihara, 2014: Assessment of offshore wind energy potential
359 using mesoscale model and geographic information system. *Renewable Energy*,
360 **69**, 506-515.

361

362

363 **List of Tables**

364 Table 1. Model configuration.

	Domain 01	Domain 02
Model	WRF V3.5.1	
Initial/boundary condition	NCEP Final (FNL) reanalysis data	
Simulation period	2006 Jan 01 – 2015 Dec 31	
Grid spacing	30 km	10 km
Number of grids	150 x 150	220 x 214
Number of vertical layers	38 layers	
Microphysics scheme	WRF single-moment 6-class scheme	
Land surface scheme	Noah land-surface model	
Boundary layer scheme	Yonsei university scheme	
Shortwave radiation	Dudhia scheme	
Longwave radiation	RRTMG Longwave scheme	
Cumulus	Kain-Fritsch scheme	

365

366

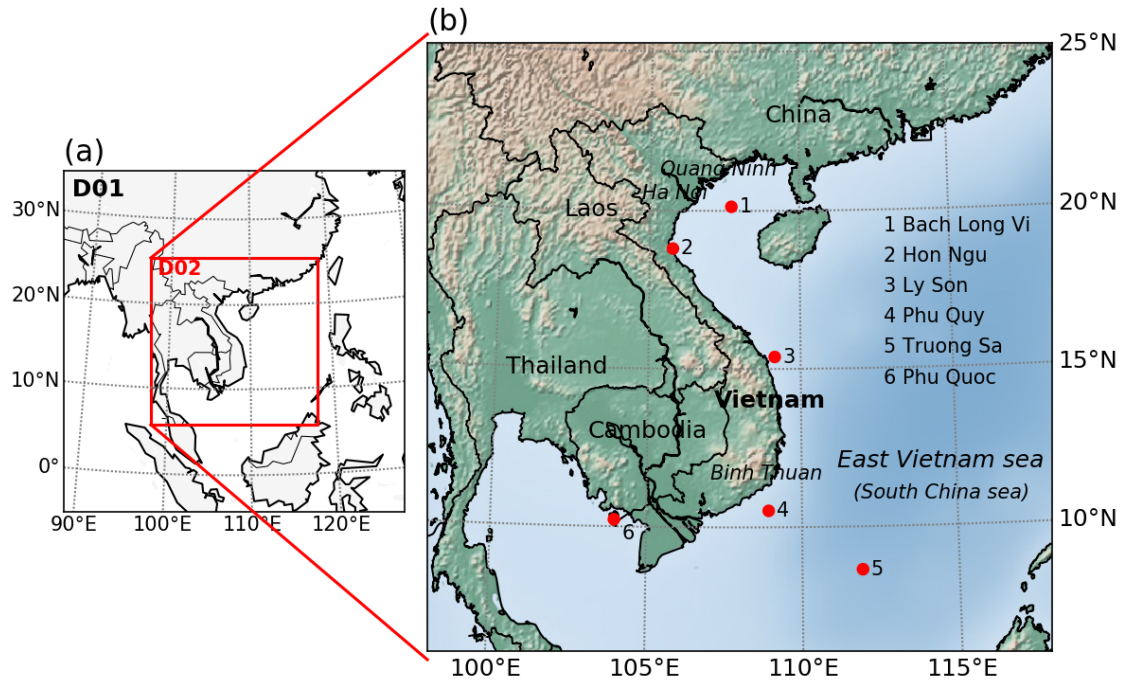
367 Table 2. List of ground-based weather stations

Station	Latitude	Longitude	Model land use	Wind speed bias (m/s)
Bach Long Vi	20.13	107.72	Water surface	2.2
Hon Ngu	18.8	105.77	Water surface	3.1
Ly Son	15.38	109.15	Water surface	2.5
Phu Quy	10.52	108.93	Water surface	3.5
Truong Sa	8.65	111.92	Water surface	1.3
Phu Quoc	10.22	103.97	Forest (evergreen broadleaf)	0.9

368

369

370 List of figures

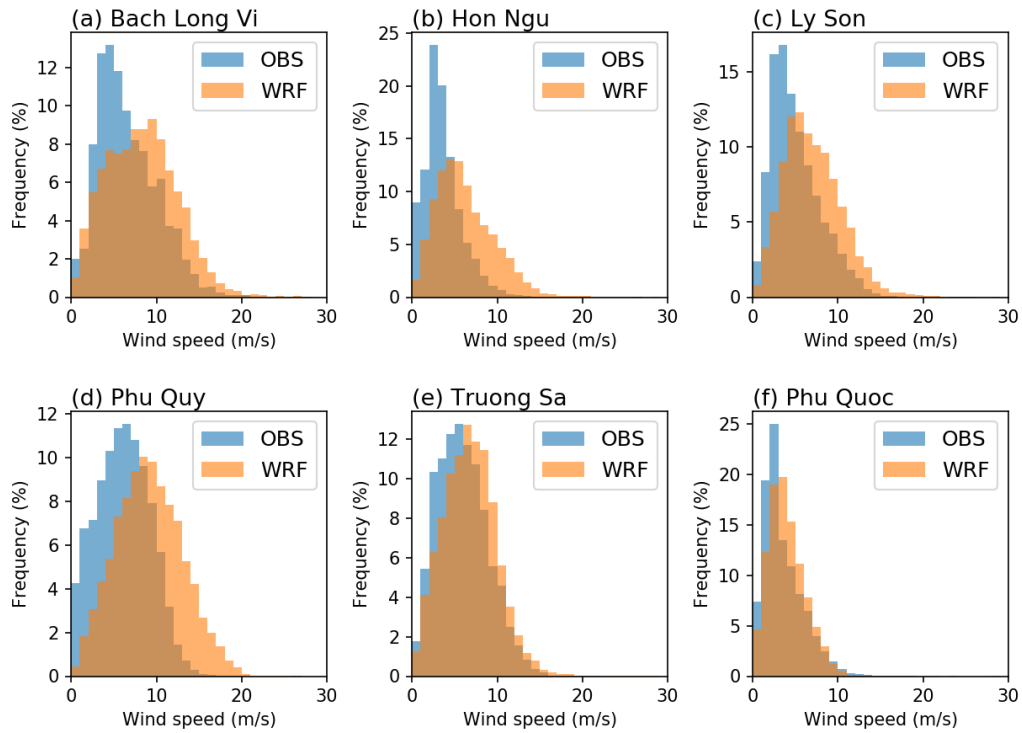


371

372 Fig. 1. (a) Configuration of the WRF domains. D01 and D02 stands for domain 01 and 02, having
373 horizontal resolutions of 30 and 10 km, respectively. (b) Detailed map for D02. Red circle markers
374 indicate the location of ground based weather stations in offshore islands of Vietnam. Wind data
375 from such stations are used for validation of the WRF model.

376

377



378

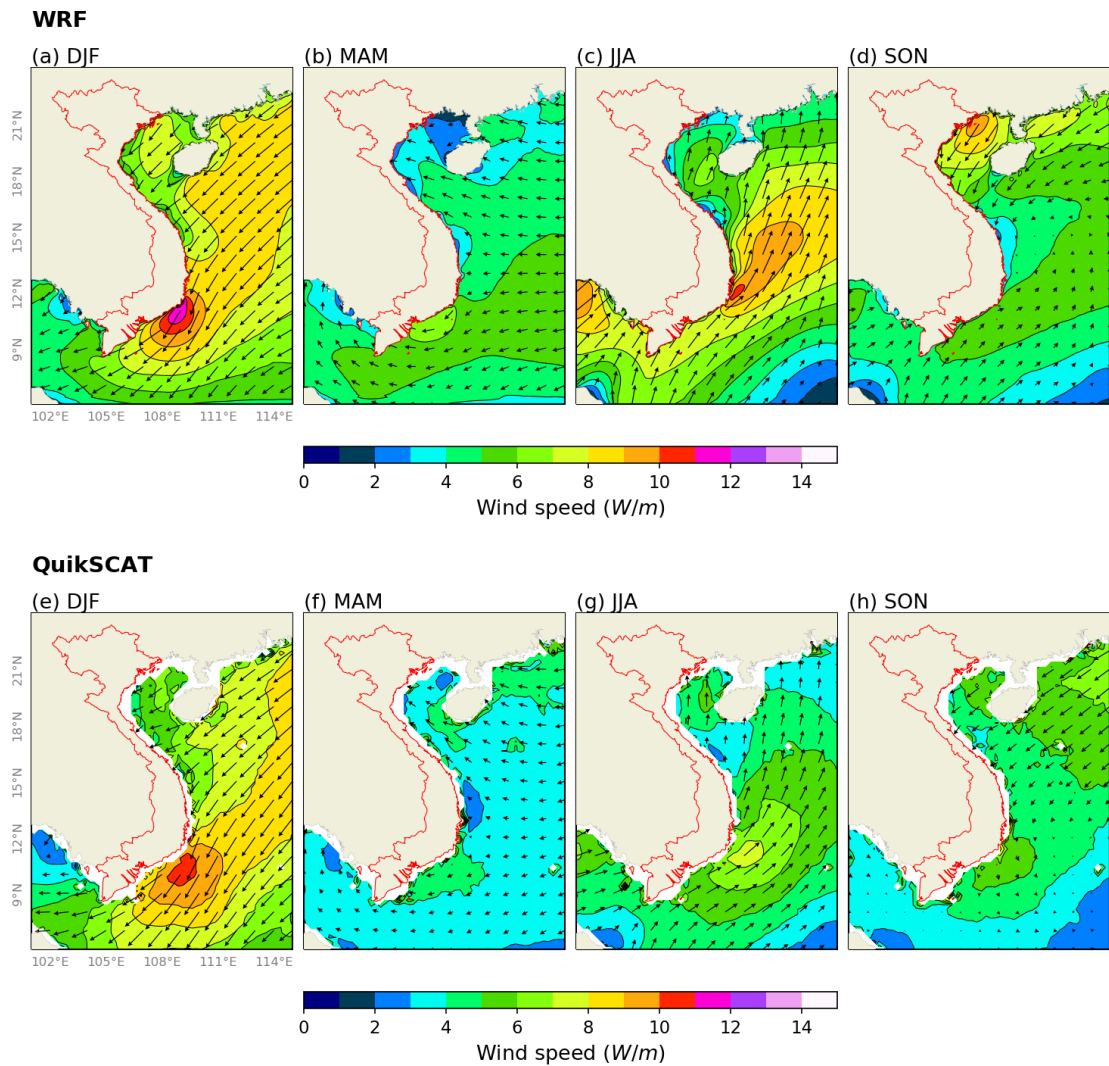
379 Fig. 2. Probability distribution of the simulated (WRF) and observed (OBS) surface wind speed
380 data at six stations. Data are four times per day (00, 06, 12, and 18 UTC) for 10 years 2006 –
381 2015.

382

383

384

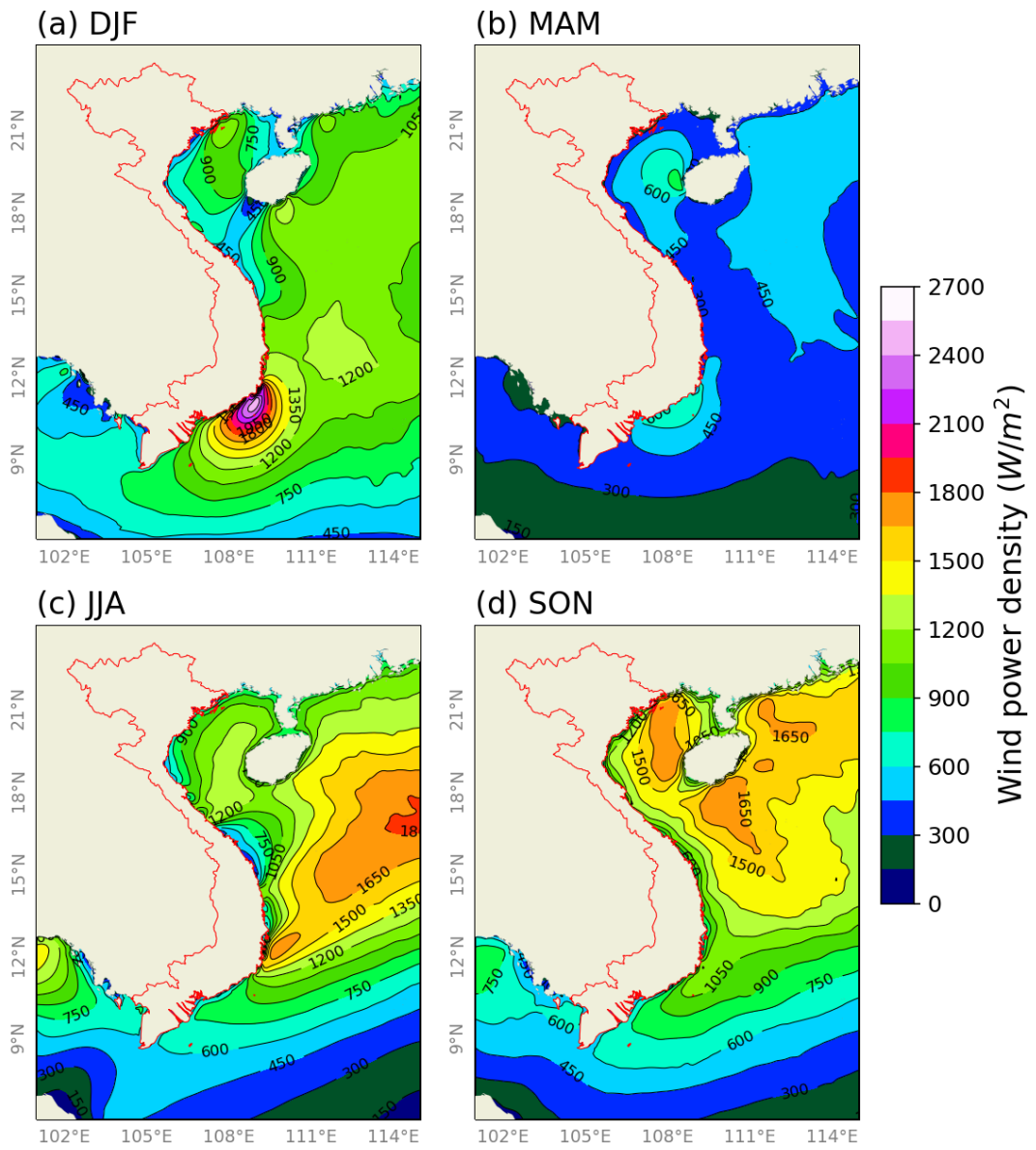
385



386

387 Fig. 3. Spatial distribution of seasonal mean surface wind speed from the WRF and the
388 QuikSCAT data. Data was averaged for five years 2006 – 2010.

389

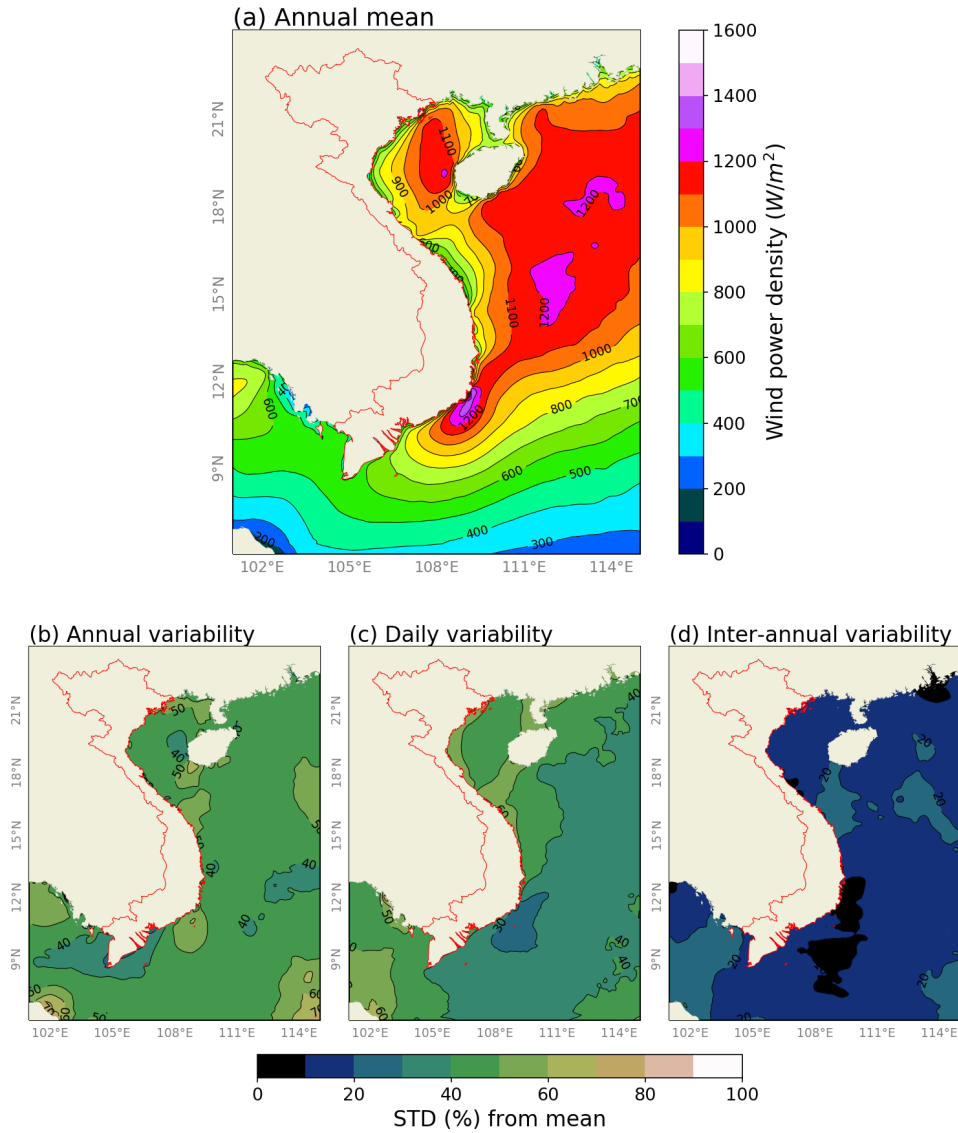


390

391 Fig. 4. Spatial distribution of seasonal mean wind power density calculated at the hub height.

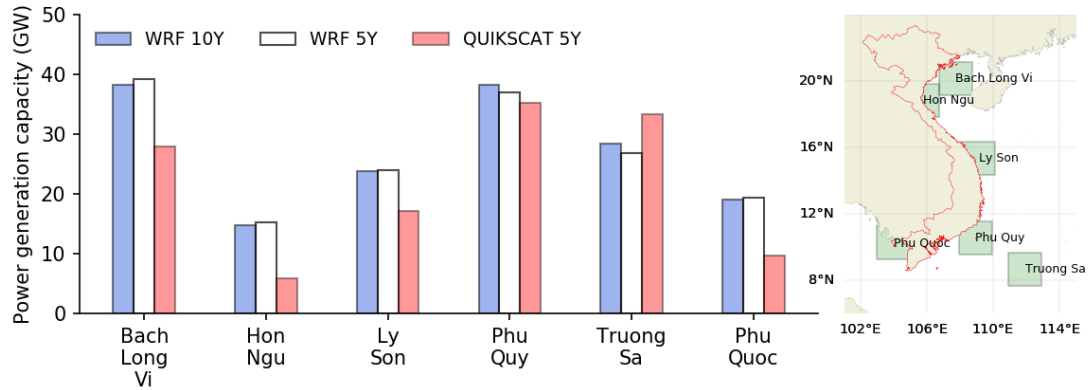
392

393



394 Fig. 5. (a) Spatial distribution of the annual mean wind power density at the turbine hub height;
 395 (b) seasonal variability, defined as the normalized standard deviation of the monthly mean values;
 396 (c) daily variability, defined as the normalized standard deviation of hourly data; (d) inter-annual
 397 variability, defined as the normalized standard deviation of yearly mean from 10-year mean.

398



399

400 Fig. 6. Power generation capacity in areas of 6 islands. The power capacity is integrated by entire
401 offshore area (within the box of 200 x 200 km) assumed hypothetical turbine Vestas V164-8.0
402 and the maximum 2 turbines is installed into 1 km². WRF 10 Y represents the 10-year (2006 –
403 2015) mean WRF data; WRF 5 Y and QUIKSCAT 5 Y are the 5-year (2006 – 2010) mean of
404 WRF and QuikSCAT data, respectively.

405